Effect of Aluminum Oxide Nanoparticles on the Mechanical Properties of Natural Rubber/Styrene–Butadiene Rubber Blends Reinforced with Carbon Black and Titanium Dioxide Nanoparticles

Zaid Ghalib Abdulkadhim Al-Jlaihawi*, Suadad Noori Ghani, Muna Hameed Alturaihi

Department of Mechanical Engineering, Faculty of Engineering, University of Kufa, Najaf, Iraq
*Email: zaidgh.abdulkadhim@uokufa.edu.iq

Abstract:

This study investigated the reinforcing effect of aluminum oxide and titanium dioxide nanoparticles, used individually and as hybrid fillers, on the mechanical performance of natural rubber/styrene–butadiene rubber vulcanizates reinforced with carbon black. The composites were fabricated by conventional compounding and compression molding following ASTM standards. Mechanical performance was evaluated through tensile strength, compression set, hardness, and scanning electron microscopy. A total of 100 specimens were prepared and classified into two groups according to nanoparticle loading. The results demonstrated that hybrid incorporation of aluminum oxide and titanium dioxide nanoparticles produced superior reinforcement compared with the use of titanium dioxide alone. The optimum formulation, containing 10 parts per hundred rubber of aluminum oxide and 8 parts per hundred rubber of titanium dioxide, achieved the highest tensile strength of 27.93 ± 0.71 MPa and the maximum hardness of 72 ± 5 International Rubber Hardness Degrees. The lowest compression set (19.65 ± 1.60%) was obtained with titanium dioxide alone, whereas the hybrid system maintained a low compression set (24.66 ± 1.30%) while simultaneously providing substantial improvements in tensile strength and hardness. Scanning electron microscopy revealed a uniform nanoparticle distribution with limited agglomeration and good interfacial adhesion, explaining the enhanced mechanical behavior. These findings demonstrate that hybrid aluminum oxide–titanium dioxide nanoparticles are effective reinforcing fillers for high-performance rubber composites.

Keywords:

NR/SBR blend, alumina, Titania, Hybrid nanocomposites, Carbon blacks, Tensile strength.

1. Introduction

Elastomeric materials, whether natural rubber (NR) or synthetic rubber, can be processed and shaped like viscous fluids [1]. Cross-linking of polymer chains is achieved through vulcanization, which transforms the viscous material into an elastic solid [2]. Natural rubber offers excellent tensile strength and fatigue resistance, while styrene-butadiene rubber (SBR) provides better abrasion resistance, aging stability, and lower cost. Blending NR with SBR combines the advantages of both: high resilience and tear strength from NR, together with improved wear resistance and weathering durability from SBR. Therefore, NR/SBR blends are widely used in tire treads, conveyor belts, hoses, and automotive components. To further enhance mechanical properties, such as tensile, compressive, and fatigue strengths, stiffness, and hardness, natural rubber has traditionally been reinforced with carbon black (CB) or silica [3,4]. These conventional fillers improve strength by forming a filler network that restricts polymer chain mobility and distributes stress. However, CBs and silica have limitations, including high energy consumption during mixing, poor dispersion at high loadings, and negative environmental impacts [4]. In recent years, further improvements in elastomer properties have been achieved by adding nano-sized fillers [5]. Due to their extremely high surface area-to-volume ratio, nanomaterials used as fillers can significantly increase the interaction strength within the polymer matrix, leading to enhanced thermal, electrical, and mechanical properties compared to conventional micro-sized fillers [6]. Nano-filler such as SiO_2 [7–9], $CaCO_3$ [10,11], clay [12,13] have been employed to produce high-performance rubbers with excellent mechanical properties. For example, nano-silica improves tear strength and reduces heat build-up, while nano-clay enhances barrier properties. Nevertheless, research on these fillers remains debated. The primary challenge is controlling the microstructure of the produced materials, including achieving uniform nanoparticle dispersion, preventing agglomeration, and ensuring strong filler-rubber interfacial adhesion. Poor dispersion leads to stress concentration points and reduced mechanical performance, negating the benefits of nano-scale reinforcement. Al_2O_3 (alumina) and TiO_2 (titania) are widely used as fillers in various polymers, including elastomers and rubbers, because they improve physical and mechanical properties. Alumina is hard, thermally conductive, and provides high modulus and abrasion resistance. Titania offers UV shielding, photocatalytic activity, and moderate reinforcement. Adding these fillers to a rubber matrix strengthens mechanical performance and increases efficiency [14–18]. In most studies on rubber reinforced with nanoparticles for various applications [19–25], nano-fillers have been used individually to strengthen rubber vulcanizates. For instance, Ch Yeswin et al. [18] investigated the physical properties of SBR/NBR rubber blends reinforced with nano-Al_2O_3 at four different loadings (1, 3, 5, and 7 phr), using silica filler instead of CBs. They reported improvements in modulus and hardness with increasing Al_2O_3 content. Naphon et al. [26] examined the effect of TiO_2 nanoparticle content (0 phr, 0.1–1.0 phr, 10 phr, and 20 phr) on the thermal, electrical, and mechanical properties of natural rubber, reporting that nano-titania enhances mechanical properties, particularly at low loadings due to better dispersion. However, single nano-fillers often cannot simultaneously improve all target properties. For example, high Al_2O_3 loading increases hardness but may worsen compression set (i.e., reduce elastic recovery). High TiO_2 loading improves UV resistance but can lead to agglomeration, reducing tensile strength. This trade-off suggests that hybrid systems may offer synergistic benefits. A few studies have explored hybrid filler systems in rubber composites. Dakhil et al. [27] and Al-Waily et al. [28] used a hybrid of SiO_2 and Al_2O_3 as reinforcements in composite materials, observing improved mechanical properties compared to single fillers. Fu [17] studied the mechanical properties of natural rubber reinforced with a combination of CBs and Al_2O_3 nanoparticles, noting that the hybrid system provided better overall performance than CBs alone. In a recent study, Njim et al. [29] developed a natural rubber method that uses graphene nanoparticles chemically bonded with local kaolin. Thus, most researchers agreed that the nature, composition, and preparation of the polymer matrix, in particular rubber, and the nanofillers strongly impact the properties of nanocomposites [30–34]. Despite the known reinforcing effects of individual Al_2O_3 and TiO_2-

nanoparticles, no study has systematically investigated their hybrid incorporation into an NR/SBR blend. Furthermore, a direct comparison between individual and hybrid filler systems in the same rubber matrix is missing. Most importantly, no optimization framework exists to balance the trade-offs between tensile strength, compression set, and hardness when using such hybrid fillers.

This study investigates three types of rubber nanocomposite blends based on NR/SBR filled with carbon blacks and $\boldsymbol{Al_2O_3}$-TiO_2 nanoparticles, using both individual and hybrid incorporation methods. The specific aims are: 1) To evaluate the reinforcement effect of individual $\boldsymbol{Al_2O_3}$ and TiO_2, and hybrid $\boldsymbol{Al_2O_3}$-TiO_2 nanoparticles on the tensile strength, compression set, and hardness of NR/SBR vulcanizates. 2) To compare the performance of single-filler versus hybrid-filler systems at different loadings. 3) To determine the best filler composition (total loading and $\boldsymbol{Al_2O_3}$: TiO_2 ratio of 2:3, 4:5, 6:7, and 8:10) for simultaneously maximizing tensile strength and hardness while minimizing compression set.

2. Materials and methods

Elastomers/rubbers employed in this study, namely NR (Natural Rubber RSS) and SBR (Styrene-Butadiene), were provided by the public tire company Babylon in Najaf, Iraq. In addition, carbon black (N330) and the other filler materials listed in Table 1 were provided by the same company. Meanwhile, the titanium dioxide nanoparticles (TiO_2) and aluminum oxide nanoparticles ($\boldsymbol{Al_2O_3}$) were used in this study, with purities of 99.5% and 99.9%+, respectively, and sizes of 50-90nm and 20nm, respectively (supplied by SkySpring Nanomaterials, Inc., USA). Rubber specimens for mechanical testing (tensile strength, compression set, and hardness) were fabricated using a mixing process. The rubber compounds used are listed in Table 1. A two-roll mill was employed to begin the mixing process. The temperature was maintained at approximately 70 ± 5 °C, as specified in ASTM D 3184-89, as shown in Fig. 1.

Fig. 1. Schematic of NR/SBR nanocomposites fabrication and images of the sheet and samples of pre-post tensile testing.

Table 1. A formulation of the NR/SBR blend compound

Compounds name	Parts per Hundred Rubber
NR	50
SBR	50
Zinc oxide	5
Streaic Aid	2
Carbone black CBS (N330)	50
Fillers*	Parts per Hundred Rubber
P-oil	4
2-(4-morpholinothio)benzothiazole	0.8
Sulphur	1.8
N-(1,3-dimethylbutyl)-N´-phenyl-p-phenylene diamine	3.25

*According to Table 2

Alumina and titania nanoparticles were introduced into the NR/SBR blend using two methods: 1) single-filler method: either alumina or titania was added alone as the filler material. 2) hybrid method: both alumina and titania were incorporated into the rubber blend. Different filler loadings were used for each method, as summarized in Table 2.

Table 2. Fillers loading (phr)

	Samples	Nano- Al_2O_3	Nano-TiO_2
1	N/SB	-	0
2	N/SB-Ti2	-	2
3	N/SB-Ti4	-	4
4	N/SB-Ti6	-	6
5	N/SB-Ti8	-	8
6	N/SB	0	0
7	N/SB-Al3-Ti2	3	2
8	N/SB-Al5-Ti4	5	4
9	N/SB-Al7-Ti6	7	6
10	N/SB-Al10-Ti8	10	8

3. Mechanical Properties testing

3-1- Tensile test

Tensile testing was performed according to ASTM D412; a tensile tester (Tensilmete) was used at room temperature with a crosshead speed of 500 mm/min. The test samples sheet can be formed by compression molding at 150°C and 35 MPa (350 bars), according to ASTM D3182, with a cure time of 45 minutes. For the tensile experiment, the specimens were prepared by cutting a 2 mm-thick molding rubber sheet, which was then formed into dumbbell shapes. The dumbbell length and width were around 33±2 and 6.3±0.1mm, respectively.

3-2- Compression test

The compression test specimens can be formed in accordance with ASTM D396 (Test Method B) by compressing the mold to 350 bars at 150°C for 20 min, as per ASTM D3182. The compression device used in this study consists of two flat steel plates on which the specimen can be compressed; the plates are sufficiently thick to withstand the compressive stresses without bending. Therefore, the compression set C% can be calculated by assessing the percentage of the original deflection as follows:

$$\text{Compression set C\%} = \frac{T_o - T_i}{T_o - T_n}\ 100\% \quad (1)$$

\mathrm{Compression\ Set}\; C(\%)=\frac{T_o-T_i}{T_o-T_n}\times100

Where;

T_o = Original thickness of the rubber specimen

T_i = Final thickness of the rubber specimen, i.e., recovered thickness.

T_n = Thickness of the spacer bar used, i.e., compressed thickness.

3-3- Hardness test

The test specimens for hardness were formed by compressing a mold at 350 bars for 15 min at 150°C, according to ASTM D 3182. Hardness is tested with a simple device called a rubber hardness tester, which has a small needle, a calibrated scale for measuring hardness in units of [IRHD] (International Rubber Hardness Degrees), and a small weight on top of the needle. By pressing a needle into the sample, the sample is placed on the device's platform at the bottom, and the needle descends into the sample, recording the meter reading at the top of the device in units [IRHD].

3-4- Scanning Electron Microscopy (SEM)

The selected samples were coated with gold using a Quorum Q300T-T turbo-pumped coating system, which permits the deposition of layers between 2nm and 20nm to increase surface conductivity and inhibit charging. The samples are now ready for SEM testing. The morphological images for these samples were obtained by using an SEM instrument (FEI QuantaTM 650 3D FEG/FIB ESEMTM.

4. Results and Discussion

4-1- Tensile stress and strain

Break stress and break strain values are recorded for five samples, and the final value is the average of these samples. The findings exhibited the tensile strength behavior (break stress MPa and break strain %) of NR/SBR blend with two filling processes and different fillers loading, as shown in Table 3 and Fig. 2. Generally, an increase in the percentage of fillers loading exhibited an increase in the stress strength and break strain as expected, as shown in Fig. 2 (blue and red lines). However, the samples containing $\boldsymbol{Al_2O_3}$-TiO_2 hybrid nanoparticles exhibit a higher maximum stress than those containing only TiO_2 nanoparticles. N/SB-Al10-Ti8, which contains 10 phr of nano-$\boldsymbol{Al_2O_3}$ and 8 phr of nano-TiO_2, had the highest break stress at 27.931+0.709 MPa, followed by the N/SB-Al7-Ti6 sample, which reached 27.475+0.854 MPa. On the other hand, the maximum break stress for the sample containing only TiO_2 nanoparticles is 22.833±0.75, in which there is a difference in stress of ~ 5 MPa, which could be attributed to the strengthening of the interaction between $\boldsymbol{Al_2O_3}$ nanoparticles and carbon black, driven by their microstructure, which prompted an extension of the mechanical behavior. Interestingly, the samples containing nano-$\boldsymbol{Al_2O_3}$ at 5 phr or above showed a significant increase in tensile strength (break stress and break strain), reaching twice the value of those below 5 phr. Hence, it could be concluded that TiO_2 with $\boldsymbol{Al_2O_3}$ nanoparticles are scattered in the cross-linked natural rubber NR strengthened SBR matrix, resulting in this matrix positively interacting with the TiO_2 and $\boldsymbol{Al_2O_3}$ nanoparticles simultaneously, where they are in link, which is consistent with Hayeemasae et al. [35], stated that the elongated shape of TiO_2 nanoparticles could effectively adsorb molecular chains under thermal conditions, thereby increasing the contact distance with the natural rubber molecular chains. Therefore, the NR matrix chains are less decomposed, and the thermal stability of natural rubber is enhanced by the collaborative interfacial adhesion of natural rubber with titania nanoparticles reinforced with alumina nanoparticles, which shows that the rubber matrix reinforced with nano-TiO_2 and nano-$\boldsymbol{Al_2O_3}$ exhibits a significant enhancement in mechanical properties compared to nano-TiO_2 alone as a filler.

Table 3. Findings of break stress, break strain, compression set, and hardness for NR/SBR blend with different loading of Al_2O_3 and TiO_2 nanoparticles. The values are calculated via mean±std. deviation.

Samples	Break stress (MPa)	Break strain% Mean (MPa)	Compression set %	Hardness IRHD
N/SB	18.536±0.98	504±5.21	25.6±2.2	62±4
N/SB-Ti2	20.233±0.872	510±6.2	24.54±2.5	62±6
N/SB-Ti4	21.88±0.541	515±5.1	22.96±3	66±5
N/SB-Ti6	22.222±0.439	521±4.7	20.87±1.5	68±3
N/SB-Ti8	22.833±0.75	525±5.6	19.65±1.3	69±3
N/SB	18.536±0.98	504±5.21	25.6±2.2	62±4
N/SB-Al3-Ti2	23.175±0.837	515±3.2	25.2±2.5	65±5
N/SB-Al5-Ti4	25.231±0.661	520.2±5.1	24.96±2	67±6
N/SB-Al7-Ti6	27.475±0.854	537±4.7	24.78±1.5	69±4
N/SB-Al10-Ti8	27.931±0.709	555.6±5.6	24.66±1.3	72±5

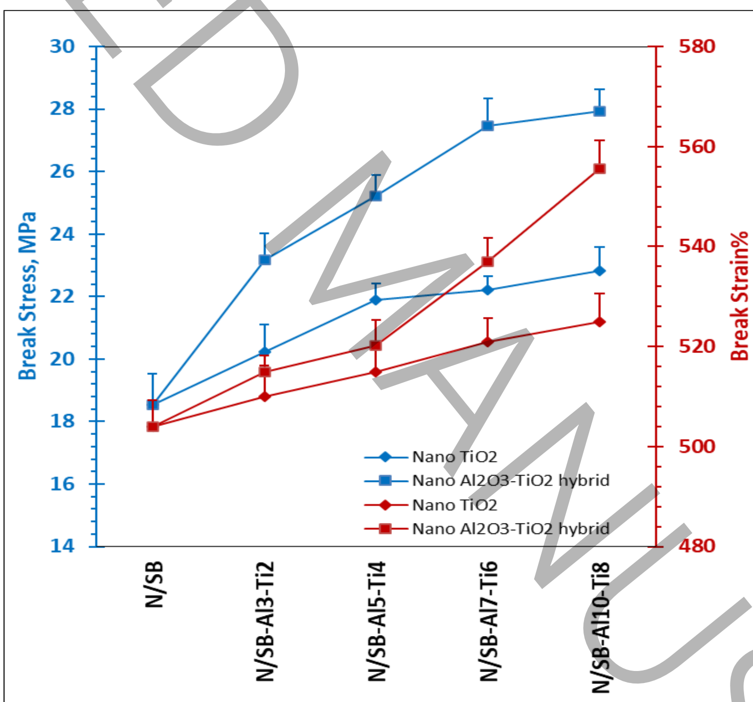

Fig. 2. Break stress and strain for NR/SBR blend with Al_2O_3 and TiO_2 nanoparticles loading.

4-2- Compression set

Fig. 3 represents the results of the compression set of NR/SER reinforced Al_2O_3 and TiO_2 nanoparticles. The compression set, C%, decreased proportionally with increasing percentages of Al_2O_3 and TiO_2 nanoparticles. The minimum compression set (C%) was observed at N/SB-Ti8, with a value of 19.65±1.6%.

Interestingly, this is in contrast to the tensile behavior shown in Table 3 and Fig. 3, which revealed that tensile stress increases with increasing percentages of $\boldsymbol{Al_2O_3}$ and TiO_2 nanoparticles. However, adding nano-$\boldsymbol{Al_2O_3}$ can enhance the compression set C% to 24.66±1.3% in the N/SB-Al10-Ti8 sample.

The hybrid filler system demonstrated a highly favorable synergistic effect, simultaneously enhancing the tensile strength, hardness, and compression set resistance of the rubber blend. Specifically, the compression set decreased from 25.6±2.2% to 24.66±1.3%, indicating superior dimensional stability under static load, as shown in Table 3. The unique architecture of the hybrid network governs this uniform improvement across different deformation modes. In tensile and indentation modes, the well-dispersed fillers act as rigid reinforcements, restricting chain slippage and increasing hardness and tensile strength. Conversely, under compressive loading, this interconnected hybrid network functions as a localized mechanical spring system [36]. The strong interfacial bonding between the hybrid fillers and the polymer matrix allows for efficient energy storage during compression, preventing macromolecular relaxation and permanent deformation. Upon removal of the compressive strain, this stored elastic energy drives rapid and complete dimensional recovery of the matrix, thereby reducing compression set, which demonstrates that the hybrid system successfully bridges the typical trade-off between material rigidity and elasticity [37].

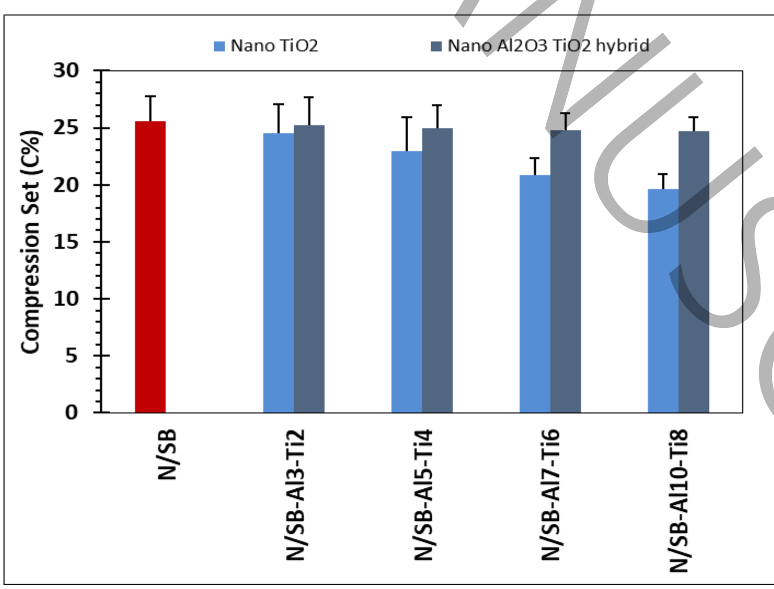

Fig. 3. Compression set for NR/SBR blend with Al_2O_3 and TiO_2 nanoparticles loading.

4-3- Hardness

The hardness findings showed that the NR/SBR samples can withstand surface scratching. Hardness values are recorded from five readings at different points on the sample's surface, and the final hardness value is the average of these readings. Generally, when filler loading percentages were enriched, the hardness value was increased as expected, as shown in Table 3 and Fig. 4. The samples containing $\boldsymbol{Al_2O_3}$-TiO_2 hybrid nanoparticles have a maximum hardness in comparison to the samples containing only TiO_2 nanoparticles. N/SB-Al10-Ti8, containing 10 phr of nano-$\boldsymbol{Al_2O_3}$ and 8 phr of nano-TiO_2, had the highest hardness, reaching 72±5 IRHD. It is slightly higher than the N/SB-Ti8 sample, amounting to 69±3 IRHD. This behavior is similar to tensile behavior and unlike the compression-set findings, as demonstrated in Figs. 2 and 3. The NR/SBR's superior mechanical behavior, reinforced with alumina and titania hybrid nanoparticles, and particularly its impact on surface resistance, could be attributed to the microstructure and ordering of the cross-linked NR/SBR matrix, with both nanoparticles used in this study. SEM images can reveal alumina and titania nanoparticles and the range of their overlap in the rubber matrix, which could inhibit surface crack propagation. In contrast, the NR/SBR blend is reinforced with only titania nanoparticles.

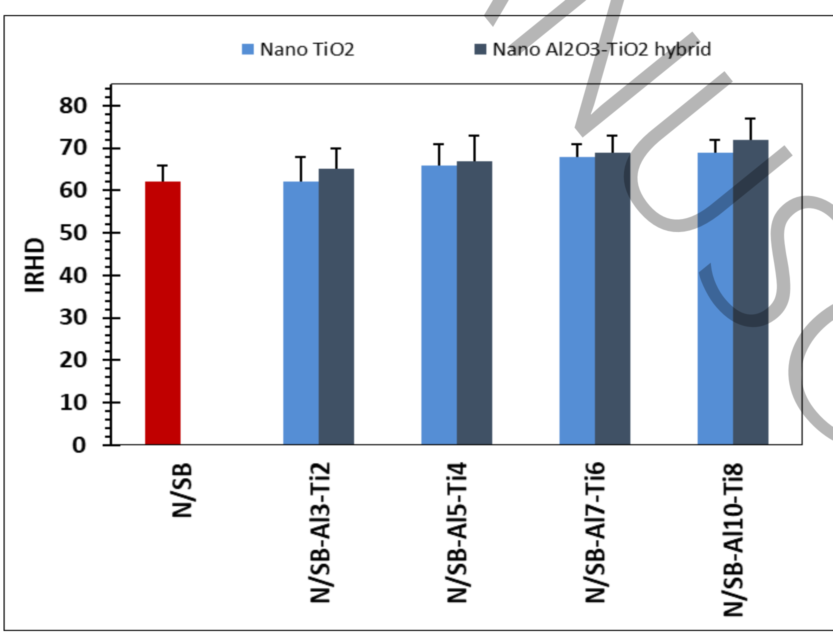

Fig. 4. Hardness [IRHD] for NR/SBR blend with $\boldsymbol{Al_2O_3}$ and TiO_2 nanoparticles loading.

4-4- Scanning Electron Microscopy (SEM)

The electron microscope was employed in this work to investigate and identify alumina and titania nanoparticles and the range of overlap in the rubber matrix. Fig. 5 illustrates the shapes of alumina nanoparticles, which range from 90 nm to 60 nm. On the other hand, as could be seen from the scanning electron microscopy, the titania nanoparticles were of a shape. These particles appeared to have a regular size and shape that overlapped in the rubber matrix, with a size of ~20 nm, as shown in Fig. 5. This is because the N/SB-Al10-Ti8 sample showed the best tensile strength and hardness among the samples. Thus, the N/SB-Al10-Ti8 sample showed the best tensile strength and hardness among the samples. Fig. 5 presents a scanning electron microscopy (SEM) image of the N/SB-Al10-Ti8 sample at a magnification of 2000X. The image reveals the dispersion state of the hybrid Al_2O_3–TiO_2 nanoparticles within the NR/SBR matrix. Most nanoparticles appear as individual particles or small clusters (< 1 μm in diameter). Large agglomerates (> 1 μm) are rare. However, high nanoparticle loadings often induce filler agglomeration, which strongly influences the composite's ultimate properties [38]. The interface between the nanoparticles and the rubber matrix appears intact, without gaps or pull-out holes, suggesting good interfacial adhesion. On the other hand, the particles are spread evenly across the field of view, with no preferential accumulation in one region, and the average inter-particle distance is estimated to be approximately 0.1–1.0 μm. These features are attributed to the filler system's hybrid nature. $\boldsymbol{Al_2O_3}$ and TiO_2 nanoparticles mutually inhibit each other’s agglomeration during mixing, resulting in a dispersion quality that is rarely achieved with single nano-fillers at similar loadings [39].

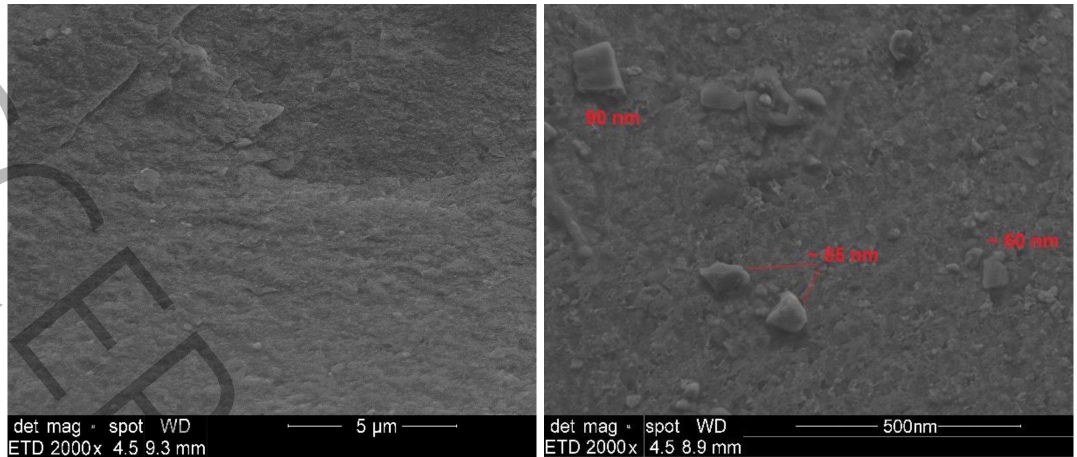

Fig. 5. The SEM images of the N/SB-Al10-Ti8 sample.

As shown, different materials at the nano- and micro-scale, including natural rubber, synthetic rubber, metallic nanoparticles, and graphene nanoplatelets, have been integrated into industrial and medical applications [40–42]. One of the limitations of this study is the absence of statistical analysis e.g., ANOVA or t-test). Future investigations should employ this kind of analysis. Other limitations of the present study include the full elemental analysis (EDS) to validate SEM interpretations. Thus, these influences should be considered in future research.

5. Conclusion

In this study, the mechanical behavior of an NR/SBR blend rubber was investigated by introducing filler materials, including carbon black as a reinforcement filler and alumina and titania nanoparticles. A mechanical methodology was applied to assess the mechanical behavior of two materials, namely $\boldsymbol{Al_2O_3}$ and TiO_2. Their mechanical behavior under different filler loading was studied by the stress-strain strength, compression set, and hardness, which were determined in order to associate their forming with their mechanical performance. It can be concluded that nano alumina and nano titania with the reinforcement filler (carbon black) have the potential to enhance the mechanical behavior of NR/SBR blend since the superior mechanical performance involving the tensile strength and the hardness was for the NR/SBR blend which was reinforced with $\boldsymbol{Al_2O_3}$ and TiO_2 hybrid nanoparticles in comparison to that using nano-titania single. On the other hand, the compression set showed a lower proportionality with the rise in the percentages of only TiO_2 and $\boldsymbol{Al_2O_3}$ and TiO_2 hybrid nanoparticles; however, a distinctive enhancement was observed for samples that were used as hybrid nanoparticles.

6. References

[1] A. Ciesielski, *An Introduction to Rubber Technology*, iSmithers Rapra Publishing, 1999.

[2] M. Akiba, Vulcanization and crosslinking in elastomers, Progress in Polymer Science, 22 (1997) 475–521. https://doi.org/10.1016/S0079-6700(96)00015-9.

[3] Q.H. Jebur, M.J. Jweeg, M. Al-Waily, H.Y. Ahmad, K.K. Resan, Hyperelastic models for the description and simulation of rubber subjected to large tensile loading, Archives of Materials Science and Engineering, 2 (2021) 75–85. https://doi.org/10.5604/01.3001.0015.0256.

[4] M.J. Jweeg, Z.G.A. Al-Jlaihawi, Characterization of natural rubber, polybutadiene rubber and styrene–butadiene rubber blends cured in a vulcanization system, Materials Science Forum, 1039 (2021) 51–64. https://doi.org/10.4028/www.scientific.net/MSF.1039.51.

[5] N.G. Sahoo, S. Rana, J.W. Cho, L. Li, S.H. Chan, Polymer nanocomposites based on functionalized carbon nanotubes, Progress in Polymer Science, 35 (2010) 837–867. https://doi.org/10.1016/j.progpolymsci.2010.03.002.

[6] S. Thomas, R. Stephen, *Rubber Nanocomposites: Preparation, Properties, and Applications*, John Wiley & Sons, 2010.

[7] K. Pal, R. Rajasekar, D.J. Kang, Z.X. Zhang, S.K. Pal, C.K. Das, J.K. Kim, Effect of fillers on natural rubber/high-styrene rubber blends with nanosilica: morphology and wear, Materials & Design, 31 (2010) 677–686. https://doi.org/10.1016/j.matdes.2009.08.014.

[8] K. Aldawoudi, A.M. Nattah, N.S. Radhi, Z.S. Al-Khafaji, M.K. Ibrahim, Identification of the microstructure and mechanical behavior of aluminum hybrid nanocomposites prepared by casting technique, Jordan Journal of Mechanical and Industrial Engineering, 19 (2025) 163–170.

[9] S. Sattar, Y. Alaiwi, N.S. Radhi, Z. Al-Khafaji, Numerical simulation for effect of composite coating (TiO_2 + SiO_2) thickness on steam turbine blades thermal and stress distribution, *Academic Journal of Manufacturing Engineering* **21** (4) (2023) 86–99.

[10] Z.G. Abdulkadhim, Influence of calcium carbonate nanoparticles on the mechanical properties of natural rubber compounds, International Journal of Mechanical and Mechatronics Engineering, 14 (2014) 114–117.

[11] S. Mishra, N.G. Shimpi, U.D. Patil, Effect of nano-$CaCO_3$ on the thermal properties of styrene–butadiene rubber, Journal of Polymer Research, 14 (2007) 449–459. https://doi.org/10.1007/s10965-007-9127-5.

[12] M. Bhattacharya, A.K. Bhowmick, Synergy in carbon-black-filled natural rubber nanocomposites. Part I: mechanical and dynamic mechanical properties and morphology, Journal of Materials Science, 45 (2010) 6126–6138. https://doi.org/10.1007/s10853-010-4699-6.

[13] R. Rajasekar, K. Pal, G. Heinrich, A. Das, C.K. Das, Development of nitrile–butadiene rubber–nanoclay composites with epoxidized natural rubber as a compatibilizer, Materials & Design, 30 (2009) 3839–3845. https://doi.org/10.1016/j.matdes.2009.03.014.

[14] A. Buzarovska, Polylactic-acid nanocomposites with functionalized titanium dioxide nanoparticles, Polymer-Plastics Technology and Engineering, 52 (2013) 280–286.

[15] S.S. Al-Taweel, H.R. Saud, A.A.H. Kadhum, M.S. Takriff, Influence of the titanium dioxide nanofiller ratio on the morphology and surface properties of titanium dioxide/chitosan nanocomposites, Results in Physics, 13 (2019) 102296. https://doi.org/10.1016/j.rinp.2019.102296.

[16] K. Song, Micro- and nano-fillers used in the rubber industry, in: S. Thomas, H.J. Maria (Eds.), *Progress in Rubber Nanocomposites*, Woodhead Publishing/Elsevier, 2017, pp. 41–80. https://doi.org/10.1016/B978-0-08-100409-8.00002-4.

[17] J.-F. Fu, W.-Q. Yu, X. Dong, L.-Y. Chen, H.-S. Jia, L.-Y. Shi, Q.-D. Zhong, W. Deng, Mechanical and tribological properties of natural rubber reinforced with carbon black and aluminum oxide

nanoparticles, Materials & Design, 49 (2013) 336–346. https://doi.org/10.1016/j.matdes.2013.01.033.

[18] C. Yeswin, D.B.S. Vamsi, B.N. Vijay, I. Naveen, P.S.P. Reddy, N. Rahulan, Physical properties of nano-aluminum-oxide-reinforced nitrile–butadiene rubber/styrene–butadiene rubber blends, Materials Today: Proceedings, 52 (2022) 2273–2278. https://doi.org/10.1016/j.matpr.2021.08.241.

[19] I.Q. Al Saffar, M. Al-Waily, S.G. Hussein, M.A. Al-Shammari, Life enhancement of partial removable denture made by biomaterials reinforced by graphene nanoplates and hydroxyapatite with the aid of artificial neural network, *Journal of Mechanical Engineering Research and Developments* **43** (6) (2020) 269–285.

[20] E.N. Abbas, M.J. Jweeg, M. Al-Waily, Analytical and numerical investigations for dynamic response of composite plates under various dynamic loading with the influence of carbon multi-wall tube nano materials, *International Journal of Mechanical & Mechatronics Engineering* **18** (6) (2018) 1–10.

[21] M. Al-Waily, M.H. Tolephih, M.J. Jweeg, Fatigue characterization of composite materials used in artificial socket prostheses with the addition of nanoparticles, IOP Conference Series: Materials Science and Engineering, 928 (2020) 022107. https://doi.org/10.1088/1757-899X/928/2/022107.

[22] T.S.N. Aswad, M. Al-Baghdadi, M. Al-Waily, M.A. Bin Razali, Performance enhancement of a photovoltaic cell operating under hot environmental conditions using aluminum oxide nanofluids: a computational fluid dynamics study, International Journal of Nanoelectronics and Materials, 14 (2021) 317–328.

[23] M. Mohamed, N. Fahad, M. Al-Waily, K. Resan, Investigation of rubber creep behavior with the effect of multiwalled carbon nanotube nanoparticles, International Journal of Mechanical Engineering and Technology, 9 (2018) 729–746.

[24] S.I. Salih, J.K. Oleiwi, H.M. Ali, Investigation the properties of silicone rubber blend reinforced by natural nanoparticles and UHMWPE fiber, *International Journal of Mechanical Engineering and Technology* **10** (1) (2019) 164–178.

[25] R.O. Al-Mansoori, A.A. Diwan, A.A. Taher, Influence of alumina and zinc oxide nanoparticles on the tensile, impact, and hardness properties of epoxy nanocomposites, Journal of Physics: Conference Series, 1973 (2021) 012047. https://doi.org/10.1088/1742-6596/1973/1/012047.

[26] P. Naphon, S. Wiriyasart, N. Naphon, Thermal, mechanical, and electrical properties of rubber latex containing titanium dioxide nanoparticles, Composites Communications, 22 (2020) 100449. https://doi.org/10.1016/j.coco.2020.100449.

[27] N. Dakhel, A.A. Kadhim, R.H. Al-Khayat, M. Al-Waily, Effect of silicon dioxide and aluminum oxide hybrid nanomaterials on the fatigue behavior of laminated composite materials used to manufacture artificial socket prostheses, Materials Science Forum, 1039 (2021) 493–509.

[28] M. Al-Waily, M.J. Jweeg, M.A. Al-Shammari, K.K. Resan, A.M. Takhakh, Improvement of the buckling behavior of composite plates reinforced with hybrid nanomaterial additives, Materials Science Forum, 1039 (2021) 23–41. https://doi.org/10.4028/www.scientific.net/MSF.1039.23.

[29] E.K. Njim, M.J. Jweeg, N.A. Alhilo, M.H. Almaamori, M.S.A.-D. Tahir, R. Madan, M.A. Al-Shammari, M.K. Singh, Enhancing mechanical and physical properties of natural rubber nanocomposites with classical and nanofillers: experimental and numerical modeling approach, *Discover Applied Sciences* **7** (2025) 1384. https://doi.org/10.1007/s42452-025-07970-7.

[30] P. Purushothaman, S. Masimalai, V. Subramani, Effective utilization of mahua oil blended with optimum amounts of aluminum oxide and titanium dioxide nanoparticles for improved performance in a compression-ignition engine, Environmental Science and Pollution Research, 28 (2021) 11893–11903. https://doi.org/10.1007/s11356-020-07926-x.

[31] N. Sokhandani, O. Bavi, S. Zebarjad, A. Setoodeh, Experimental investigation and semi-empirical modeling of mechanical behavior in graphene, graphene oxide, and reduced graphene oxide nanocomposites, Results in Engineering, 26 (2025) 105290. https://doi.org/10.1016/j.rineng.2025.105290.

[32] A. Mudhoo, R.K. Gautam, M.C. Ncibi, F. Zhao, V.K. Garg, M. Sillanpää, Green synthesis, activation and functionalization of adsorbents for dye sequestration, *Environmental Chemistry Letters* **17** (1) (2019) 157–193. https://doi.org/10.1007/s10311-018-0784-x.

[33] N. Sokhandani, O. Bavi, S.M. Zebarjad, A. Setoodeh, Structure–property correlations in graphene-based epoxy nanocomposites and their effect on tribological performance, Journal of Applied Polymer Science, 143 (2025) 70184. https://doi.org/10.1002/app.70184.

[34] N. Sokhandani, O. Bavi, S.M. Zebarjad, A. Setoodeh, Thermal decomposition kinetics and viscoelastic properties of epoxy nanocomposites: comparative effects of graphene, graphene oxide, and reduced graphene oxide nanoparticles, Polymer Composites, 47 (2026) 4398–4413. https://doi.org/10.1002/pc.70433.

[35] N. Hayeemasae, H. Ismail, S. Matchawet, A. Masa, Kinetics of thermal degradation and thermal stability of natural rubber filled with titanium dioxide nanoparticles, Polymer Composites, 40 (2019) 3149–3155. https://doi.org/10.1002/pc.25163.

[36] A.C. Azevedo Vasconcelos, D. Schott, J. Jovanova, Hybrid mechanical metamaterials: advances in multifunctional mechanical metamaterials with simultaneous static and dynamic properties, Heliyon, 11 (2025) e41985. https://doi.org/10.1016/j.heliyon.2025.e41985.

[37] E. Garmroudi Nezhad, F. Saba, G. Fan, Z. Tan, Z. Li, Toward overcoming the trade-off between hetero-deformation-induced hardening and strain localization: a review of micro/nano hybrid-reinforced composites, Composites Part B: Engineering, 308 (2026) 113028. https://doi.org/10.1016/j.compositesb.2025.113028.

[38] H. Ali, S. Ali, K. Ali, S. Ullah, P.M. Ismail, M. Humayun, C. Zeng, Effect of nanoparticle incorporation on the enhancement of polymer mechanical properties, Results in Engineering, 27 (2025) 106151. https://doi.org/10.1016/j.rineng.2025.106151.

[39] Y. Reches, K. Thomson, M. Helbing, D.S. Kosson, F. Sanchez, Agglomeration and reactivity of silicon dioxide, titanium dioxide, aluminum oxide, iron oxide, and clay nanoparticles in cement

pastes and their effects on compressive strength at ambient and elevated temperatures, Construction and Building Materials, 167 (2018) 860–873. https://doi.org/10.1016/j.conbuildmat.2018.02.032.

[40] M. Rahbar, O. Bavi, S. Pashangeh, M. Alizadeh, Effect of reinforcement type, size, and content on the bonding behavior of aluminum-based composites fabricated by cold-roll bonding, Ceramics International, 52 (2026) 4927–4947. https://doi.org/10.1016/j.ceramint.2025.12.268.

[41] Z.J. Wally, O.M. Al-Jubouri, Z.G. Al-Jlaihawi, R.M. Almusawi, R.A. Alamoush, J. Haider, Effects of incorporating magnesium oxide and zirconium dioxide nanoparticles into acrylic-resin denture-base material: a comparative study, Frontiers in Dental Medicine, 6 (2025) 1667644. https://doi.org/10.3389/fdmed.2025.1667644.

[42] A.R. Dhumal, A.P. Kulkarni, N.H. Ambhore, Recent developments in carbon based and graphene based thermal interface materials: a review, *AUT Journal of Mechanical Engineering* (2026). https://doi.org/10.22060/ajme.2026.24363.6196.